Carbohydrate Polymers 84 (2011) 1350–1356

Contents lists available at ScienceDirect

Carbohydrate Polymers

journal homepage: www.elsevier.com/locate/carbpol

Removal of anionic dye eosin Y from aqueous solution using ethylenediamine modified chitosan

Xiao-Yi Huang[a], Jian-Ping Bin[b], Huai-Tian Bu[c], Gang-Biao Jiang[a,*], Ming-Hua Zeng[d,*]

[a] College of Natural Resources and Environment, South China Agricultural University, Guangzhou 510642, China
[b] Department of Cardiology, Nanfang Hospital, Southern Medical University, Guangzhou 510515, China
[c] SINTEF Materials and Chemistry, P.O. Box 124 Blindern, N-0314 Oslo, Norway
[d] The Key Laboratory for the Chemistry and Molecular Engineering of Medicinal Resources (Ministry of Education), School of Chemistry and Chemical Engineering of Guangxi Normal University, Guilin 541004, China

ARTICLE INFO

Article history:
Received 29 October 2010
Received in revised form 20 January 2011
Accepted 21 January 2011
Available online 28 January 2011

Keywords:
Chitosan
Adsorption
Sorbent
Eosin Y
Chitosan derivative
Effluent treatment

ABSTRACT

In this study, chitosan was cross-linked with ethylenediamine (EDA) to prepare an outstanding sorbent for the removal of anionic dye eosin Y from aqueous solution. FTIR, DTG, XPS and zeta potential analysis were used to characterize the sorbent. The effect of particle size, solution pH, agitation rate, temperature, adsorbent dosage (50–500 mg/L), contact time (10 min–24 h) and initial concentration of dye (50–300 mg/L) on the adsorption process was investigated. Langmuir and Freundlich adsorption models were applied to describe the isotherms and isotherm constants, and the data fitted well with Langmuir model with a maximum adsorption capacity of 294.12 mg/g at 25 °C. Kinetic studies followed the pseudo second-order rate model, which indicated that the chemisorption is the rate-limiting step. Thermodynamic parameters such as enthalpy change ($\Delta H^\circ = -5.004$ kJ/mol), free energy change ($\Delta G^\circ < 0$) and entropy change ($\Delta S^\circ = -11.656$ J/(mol K)) indicate the exothermic and spontaneous nature of adsorption.

1. Introduction

The biopolymer chitin and its derivative chitosan have gained importance in environmental biotechnology due to their very good adsorption capacity towards dyes and metal ions (Crini, 2006; Figueiredoa, Loureirob, & Boaventurab, 2005; Ngah, Ab Ghani, & Kamari, 2005). Chitin is widely found in the exoskeleton of crustaceous, the cuticles of insects and the cell walls of fungi (Crini, 2006). Commercial chitin product is now primarily extracted from the exoskeleton of crustaceans (crab, krill, crayfish), an abundant by-product of food processing (Crini, 2006). Chitosan is a natural cationic polymer obtained by deacetylation of chitin. It is more efficient than chitin in terms of adsorption capacity due to the presence of a large number of free amino ($-NH_2$) groups that can serve as the coordination and reaction sites. However, chitosan is soluble in most dilute acids, limiting its utilization of adsorbent for acidic effluents. Therefore, various physical and chemical modifications have been developed to improve the chemical stability of chitosan in acid media as well as its resistance to biochemical and microbiological degradation (Ngah et al., 2005). Chemically modified sorbent not only posses better adsorption, but also has higher stability in strong acids. Meanwhile, the mechanical strength of chitosan is also improved after modification. Some of the chemical modifications like cross-linking, grafting of a new functional group and acetylation have been applied (Chiou & Li, 2003; Kyzas & Lazaridis, 2009).

The method of amination to prepare adsorbent with high adsorption capacity for anionic dye or reactive dye has been reported using rice hull as the raw material by Ong, Lee, and Zainal (2007). They found that, compared to pure rice hull, the ethylenediamine (EDA) modified rice hull had exceptional higher affinity for reactive dye through electrostatic attraction. In the present study, chemically modified chitosan was prepared by EDA grafting, which was predicted to have higher adsorption capacity towards anionic dyes (acid dyes) by introducing more amino groups. What's more, this product showed satisfactory chemical stability in acid medium, which was confirmed by the fact that it was not dissolved at all in the hydrochloride acid solution with the pH ranging from 2 to 7, while chitosan was completely dissolved in weak acid medium. Eosin Y was chosen as the model anionic dye to evaluate the adsorption capacity of EDA modified chitosan (EDA-CS).

* Corresponding author.
E-mail addresses: jgb3h@163.com (G.-B. Jiang), zmh@mailbox.gxnu.edu.cn (M.-H. Zeng).

0144-8617/$ – see front matter © 2011 Elsevier Ltd. All rights reserved.
doi:10.1016/j.carbpol.2011.01.033

2. Materials and methods

2.1. Materials

Chitosan was obtained from Sanland chemical Co, LTD (Los Angeles CA, USA), the average molecule weight was 45 kDa, and the degree of deacetylation (DD) was above 95%. Eosin Y was an acid dye purchased from Hebaochem Co, LTD (Shanghai, China). Ethylenediamine (EDA), epichlorohydrin (ECH), and other reagents used in this experiment were of analytical grade and used without further treatment.

2.2. Preparation of ethylenediamine modified chitosan (EDA-CS)

The preparation of EDA-CS was carried out with the following steps.

Step 1: preparation of chitosan gel beadsChitosan beads were prepared by dropwise addition of chitosan solution (3%, w/v) in 2% (v/v) acetic acid solution to an alkaline precipitation bath (150 mL of 0.5 mol/L sodium hydroxide aqueous solution) as described by Ngah et al. (2005). The wet chitosan beads were collected and extensively rinsed with distilled water to remove residual NaOH, and stored in distilled water for further use.
Step 2: Reaction with epichlorohydrine (ECH)Chitosan functioned as the nucleophilic reagent to attack ECH, and the amino groups of chitosan was grafted by ECH. Briefly, the chitosan gel beads obtained in the above step was suspended in 300 mL of a mixture of water–ethanol (v/v = 1:1), and then 6 mL ECH was added to the suspension. The mixture was stirred at 60 °C for 16 h and then cooled. The solid product (ECH-CS) was filtered with a filter paper and then washed each three times with ethanol and water to remove the unreacted ECH.
Step 3: Preparation of EDA modified chitosan (EDA-CS)The product got in the preceding step was suspended in 300 mL ethanol/water mixture (1:1, v/v) and then treated with 5 mL EDA. The temperature was set at 60 °C. After stirring for 24 h, the product obtained was washed each three times with water followed by ethanol and air dried. The dry product was ground and sieved size to 100–200 μm, 200–300 μm and 450–900 μm respectively.

2.3. Characterization of EDA-CS

FT-IR spectra of pure chitosan, chitosan gel beads, ECH-CS, EDA-CS and dye loaded EDA-CS were recorded with an FTIR spectrometer (Thermo FTIR-6700, Nicolet Instrument Co., USA) in the range of 4000–400 cm^{-1} using KBr pellets containing the prepared materials.

Differential Thermal Analysis (DTA) and Thermal Gravimetric Analysis (TGA) of chitosan, ECH-CS and EDA-CS were performed with a thermal analyzer (DTG-60, Shimadzu. Japan) at a heating rate of 15 °C/min from 50 °C to 600 °C under a nitrogen flow rate of 20.0 mL/min.

X-ray photoelectron spectroscopy (XPS) was recorded on a Thermo ESCALAB 250 X-ray photoelectron spectroscope using AlKα radiation (1486.6 eV, 15 kV, 150 W). To exclude any effects on the values of binding energies due to charging of the sample during the XPS analysis, all data were corrected by a linear shift such that the peak maximum of the C1s binding energy of adventitious carbon corresponded to 284.8 eV. In order to extract the surface core-level shifts and relative intensities of these components, a curve-fitting procedure was utilized. The fitting of the core-level data was performed using a nonlinear fitting procedure (Software XPSPEAK 41).

To estimate the effect of EDA on the surface charge of chitosan, a certain amount of chitosan and EDA-CS were dispersed in deionized water previously and the zeta potential values of chitosan and EDA modified chitosan were determined using Zetasizer Nano-JS94H (Shanghai Zhongchen Digital Technique Equipment Co, Shanghai, China). Triplicate measurements were carried out and the mean value was presented.

2.4. Adsorption experiments

Stock solution of eosin Y (1 g/L) was prepared in deionized water. The experimental solutions with desired eosin Y concentration were obtained by successive dilution of this stock solution with deionized water. Calibration curve of eosin Y was prepared by measuring absorbance of samples with predetermined concentrations at 516 nm (corresponding to a maximum absorbency of eosin Y) using UV–vis spectrophotometer (UV-2300, Tian Mei CO. LTD. China).

For the adsorption experiment, a known amount of sorbent and a measured volume of eosin Y solution were placed in 50 mL closed plastic bottles resistant to acid or base. The system remained under agitation in a thermostatic bath. Parameters like pH, temperature, agitation rate, adsorbent dosage and particle size, contact time and initial dye concentration were set according to the relevant adsorption studies. Duplicate measurements were carried out for each study, and the mean values are presented, the error obtained was ±2%. The adsorbent was finally separated from the solution by filtration and small amount of dye remaining in the filter is omitted. Concentration of dye in supernatant was analyzed from the linear regression equation of the calibration curve. The removal efficiency (R, %) and the amount of eosin Y adsorbed (q, mg/g) were calculated using the following equations, respectively.

$$R = \frac{100(C_i - C_f)}{C_i} \quad (1)$$

$$q = \frac{(C_i - C_f) \times V}{1000 \times W} \quad (2)$$

where C_i and C_f are the initial and final concentration (mg/L) of dye after adsorption. V is the volume (mL) of experimental solution and W is the weight (g) of the adsorbent.

3. Results and discussion

3.1. Characterizations of EDA-CS

FT-IR spectra of chitosan, chitosan gel beads, ECH-CS, EDA-CS and dye loaded EDA-CS are presented in Fig. 1. Spectrum shows the principal spectral features in chitosan. The broad band at 3380 cm^{-1} could be assigned to the axial stretching vibration of –OH superimposed to the $–NH_2$ stretching band and inter- and extra-molecular hydrogen bonding of chitosan molecules. The spectrum also exhibits the distinctive absorption bands of chitosan at 2918 cm^{-1} and 2878 cm^{-1} (C–H stretch), 1647 cm^{-1} (amide II band, C=O stretch), 1597 cm^{-1} (NH_2 bending), 1383 cm^{-1} (amide III band, C–N stretch), 1420 cm^{-1} and 1323 cm^{-1} (C–H bending), 1259 cm^{-1} (C–N stretch), 1155 cm^{-1} (bridge C–O–C stretch) and 1082 cm^{-1} (C–O stretch) (Kyzas & Lazaridis, 2009; Ostrowska-Czubenko & Gierszewska-Drużyńska, 2009). Compared to the spectrum of pure chitosan, spectrum of chitosan gel beads presents a much higher peak at 3442 cm^{-1} corresponding to the stretching vibration of O–H overlapped by N–H stretch. Besides, the C–O stretch at 1082 cm^{-1} and NH_2 bending at 1597 cm^{-1} shift to 1068 cm^{-1} and 1603 cm^{-1} respectively, as shown in spectrum b. The reason may lay in that the inter- and extra-molecular hydrogen bonding of chitosan become weaker after dissolution and precipitation process. Spectrum c is corresponding to ECH-CS. It is obvious that a new peak appears at 1458 cm^{-1}, which can be assigned to the deformation of CH_2. The peak at 3370 cm^{-1} is sharper than that

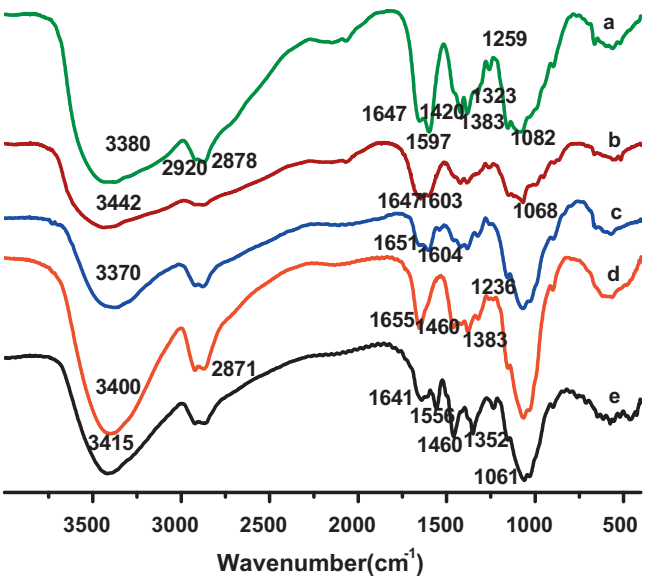

Fig. 1. FTIR spectra of chitosan (a), chitosan gel (b), ECH-CS (c), EDA-CS (d), dye loaded by EDA-CS (e).

of chitosan, suggesting the decrease of crystallinity after modification. In addition, the peak at 1259 cm^{-1} relating to the C–N stretch becomes weaker and shifts to 1255 cm^{-1}, proving the introduction reaction of ECH on the NH_2 position of chitosan. Significant changes can be found in the spectrum of EDA-CS presented in spectrum d. A more intense and narrow peak depicts at a frequency level around 3400 cm^{-1}, which indicates that a great deal of amino groups have been introduced into chitosan. Besides, the aminated chitosan shows an intense single peak at 1657 cm^{-1} overlapping the amide band of chitosan, which could be assigned to the deformation vibration of –NH in plane. Moreover, the asymmetry deformation of CH_2 at 1460 cm^{-1} and C–N stretch at 1383 cm^{-1} become stronger. Two new peaks appear at 1236 and 1261 cm^{-1}, substituting the original peak at 1259 cm^{-1} (C–N stretch), which also verify the grafting of EDA. After adsorbing eosin Y, obvious changes are observed at the frequency level of 1550–1650 cm^{-1} and 3415 cm^{-1} from spectrum e, which indicates that the primary or secondary amino groups of the EDA-CS participate in the adsorption process.

The results of the thermogravimetry/differential thermal analysis (TG/DTA) of chitosan, ECH-CS and EDA-CS were shown in Fig. 1 in Supplementary data. TGA curve of chitosan indicates that chitosan underwent weight losses at three stages. The first stage with 7.62% weight losses relates to the removal of physically adsorbed and fractional strongly hydrogen-bonded water, which could not be removed completely on drying. The second stage is the predominant stage of thermal degradation appearing in the range of 250.32 °C and 358.81 °C (with maximum at 331.37 °C), during which 35.68% decrease of chitosan mass is observed. This is caused by strong decomposition of chitosan, including dehydration of the saccharide rings, depolymerization and decomposition of the acetylated and deacetylated units of the polymer (Gao et al., 2010; Zhang, Ping, Zhang, & Shen, 2003). At the third stage, mass of chitosan drops gradually, with 24.55% residue as temperature went up to 600 °C, corresponding to further destruction of pyranose rings with ring-opening reaction and charing of chitosan by high temperature. The modification influences the thermal stability of chitosan, which can be confirmed from the TG/DTA curves of ECH-CS and EDA modified chitosan. Like chitosan, ECH-CS and EDA-CS undergo weight losses at multiple stages. The weight loss at the initial stage (<100 °C) can be assigned to the loss of water. It is obvious that the water content of the three materials was different, ECH-CS presents higher water losses (9.95%) at this stage. This may be explained by the fact that after chemical modification of the primary amino groups of chitosan, weaker hydrogen bonds forms between ECH-CS and water, which makes the water evaporation easier. This can also be proved by the thermal degradation at the second stage, where ECH-CS presented lower maximum degradation temperature at 274.41 °C, resulting from the disrupting of the crystalline structure of chitosan as a result of the modification. However, the hydrogen bonds becomes stronger again when the reaction with EDA took place, which leads to a decrease of water loss (7.35%) accompanying the increase of maximum degradation temperature at 302.07 °C.

In order to obtain additional information about the incorporation of more amine group into chitosan, XPS spectra were recorded and examined. Wide-scan XPS spectra of chitosan and EDA-CS showed three main peaks associated with the carbon, oxygen and nitrogen species. One way to detect the amine groups after modification of chitosan by EDA is by considering the N 1s spectrum of EDA-CS in comparison with the virgin chitosan. As seen from Fig. 2(a), the N 1s peak of the virgin chitosan can be fitted with one peak at 397.86 eV. The N 1s signals of EDA-CS (Fig. 2(b)), on the other hand, can be split into two peaks. One appears at the same binding

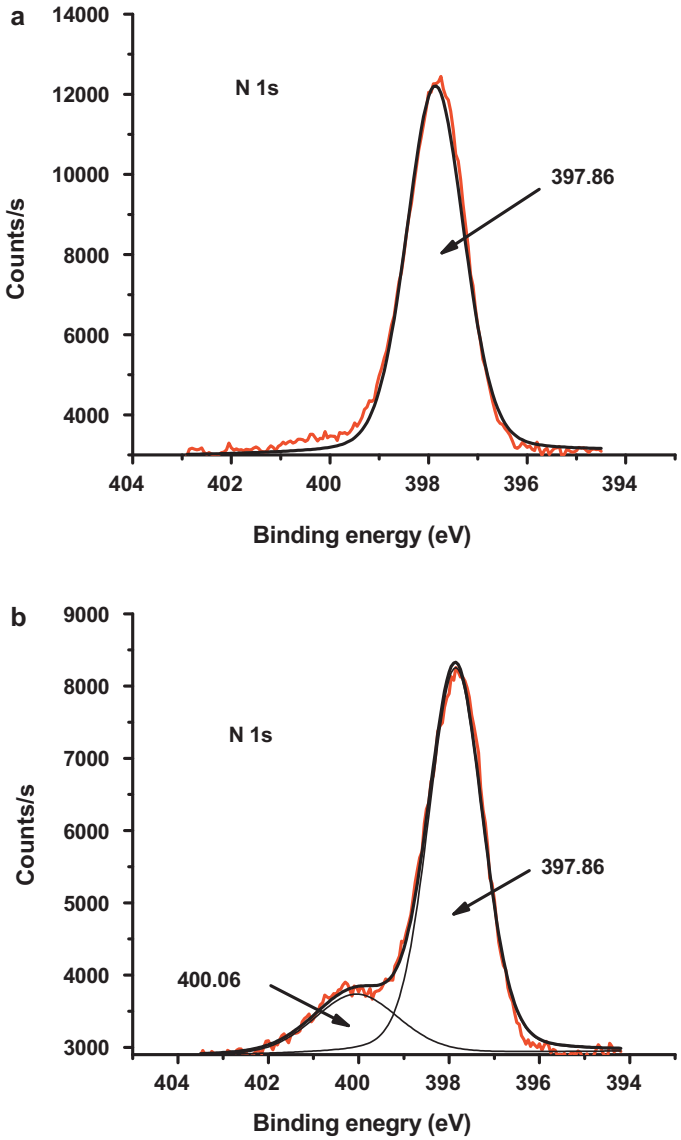

Fig. 2. XPS N 1s spectra of chitosan (a) and EDA-CS (b).

energy (397.86 eV) as chitosan. The other having higher binding energy emerges at 400.06 eV. This latter peak can be regarded as a signal from the introduction of amine group into chitosan after chemical reaction with ECH and EDA, which changed the chemical atmosphere of N 1s to some extent.

The zeta potential of chitosan and EDA-CS were 3.80 mV and 11.17 mV respectively, which indicated that both chitosan and EDA-CS were positive charged while the amino or imino groups were protonated in deionized water. What is more, the latter charged much more resulting from the introduction of more amino and imino groups. This is important for anionic dye (acid dye) adsorption as the incorporation of more amine groups would facilitate more binding sites thus increasing the adsorption capacity of chitosan.

3.2. Effect of particle size on the removal of eosin Y

The experimental condition was as following: 0.0100 g of EDA-CS beads with certain size was added in 20 mL of 100 mg/L eosin Y aqueous solution, pH of the solution was set at 5, and the mixture was equilibrated at 25 °C for 24 h under a constant shaking of 200 rpm. Results showed that the adsorption capability were 266 mg/g, 173 mg/g, 110 mg/g respectively, along with using beads of 100–200 μm, 200–300 μm, 450–900 μm as adsorbents, which indicates that larger particle size leads to lower adsorption capacity. This can be explained by the fact that the effective surface area are higher for the smaller particles comparing with that of the larger particles with the same mass, while greater particle size of the material will cause greater effect of intraparticle diffusion resistance (Crini & Badot, 2008). A similar phenomenon in relation to the adsorption of certain dyes on various adsorbents has been reported previously (Chiou & Li, 2003). In the succeeding experiments, beads with size of 100–200 μm were utilized.

3.3. Effect of pH on the removal of eosin Y

The study of the effect of acidity of dye solution on the adsorption of adsorbate onto adsorbent is fundamental, as pH strongly affects the sorption performance of the adsorbent. The experiment was carried out by measuring the dye uptake of 0.0100 g adsorbent (100–200 μm, the following experiments were carried out with the same particle size) after 2 h immersion at 25 °C. The pH of the dye solution (20 mL of 100 mg/L initial concentration) was adjusted to the range of 5–10, using either hydrochloride acid or sodium hydroxide. The adsorption of eosin Y for both adsorbents is pH dependent. As shown in Fig. 3.1, the adsorption capacity of chitosan and EDA-CS decreased drastically when pH increased from 5 to 7, and then fluctuated between pH 7 and pH 10. Similar observations of pH effect on the adsorption of anionic dyes onto chitosan and chitosan derivatives have been reported by Chiou and Li (2003), Du, Xu, Han, Xu, and Miao (2008) and Chatterjee, Lee, Lee, and Woo (2009). In the acidic solution, the adsorption process of the anionic dye eosin Y by chitosan and EDA-CS is an electrostatic interaction, where the protonated amine groups of chitosan interact with the anionic groups of the dye. While at high pH from 7 to 10, more OH^- ions present and compete with the anionic bromide groups of eosin Y for the adsorption sites of chitosan and EDA-CS, thus the available adsorption sites for anionic eosin Y decrease. Appreciable amount of adsorption in this pH range suggests involvement of physical forces such as hydrogen bonding and Van der Waals force in the adsorption process.

3.4. Effect of agitation rate on the removal of eosin Y

Agitation rate plays an important role in the adsorption process, due, that it would influence the distribution of the solute in the bulk solution and the formation of the external boundary film (Crini & Badot, 2008). This study was performed by mixing 500 mg/L of sorbent EDA-CS with 20 mL of aqueous dye solution with concentration of 100 mg/L. The mixture was shaken for 24 h in an air bath at 25 °C, pH was set at 5 and the shaking rate was adjusted to 50, 100 and 200 rpm, respectively. The eventual eosin Y uptaken by EDA-CS at three agitation rates were 113 mg/g, 182 mg/g and 199 mg/g respectively. It is clear that the adsorption of eosin Y increased with agitation rate, and a maximal adsorption is obtained under 200 rpm agitation. This may be explained by the fact that agitation reduces the boundary-layer resistance and increases the mobility of the system. Besides, increasing stirrer speed lowers the external mass transfer effect, thus promotes the intimate contact between the two phases (adsorbent and adsorbate). The agitation rate of 200 rpm was chosen for further studies since appropriate agitation rate assures that all the active sites on EDA-CS are made readily for eosin Y uptake.

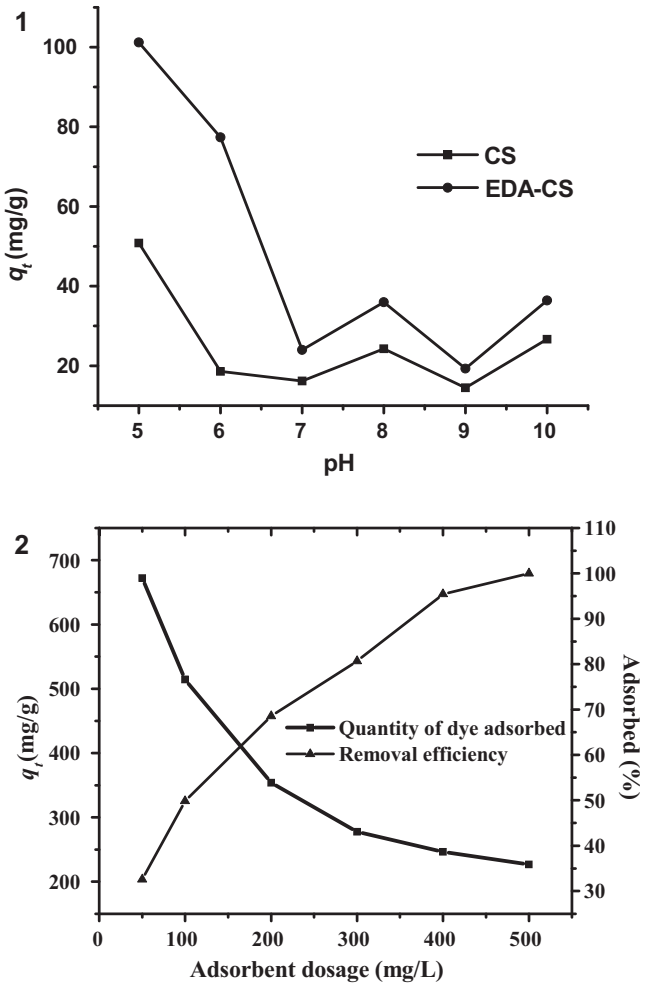

Fig. 3. Effect of pH value of dye solution (3.1) and adsorbent dosage (3.2) on eosin Y adsorption of EDA-CS.

3.5. Effect of adsorbent dosage on the removal of eosin Y

In this process, a series of experiment was carried out by varying adsorbent dosage in the range of 50–500 mg for 1 L dye solution. In 20 mL, 100 mg/L dye solution, different amounts of adsorbent ranging from 1 mg to 10 mg (corresponds to the adsorbent concentration of 50 mg/L to 500 mg/L) were charged. The pH of dye solution was set to 5, the agitation rate and temperature were adjusted to 200 rpm and 25 °C, respectively. The eosin Y uptake

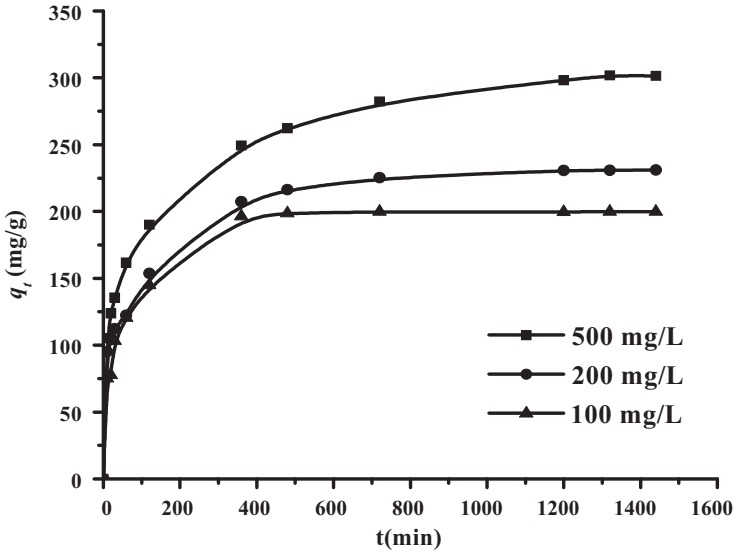

Fig. 4. Time evolution of eosin Y uptake by EDA-CS at different initial eosin Y concentrations.

amount and the removal efficiency of dye are plotted as a function of adsorbent dosage as can be seen from Fig. 3.2. It is clear that removal proportion of dyes increases with increasing adsorbent dosage, which approaches about 100% when the adsorbent dose is 500 mg/L. However, with increasing adsorbent load, the quantity of dye adsorbed onto the unit weight of the adsorbent cuts down as can be seen from the declining curve of q_t. This may be attributed to the overlapping or aggregation of adsorption sites, which leads to a decrease in total available adsorbent surface area and an increase in diffusion path length (Crini & Badot, 2008).

3.6. Effect of contact time and initial dye concentration on the adsorption of EDA-CS

In this experiment, 10 mg of sorbent was added to 20 mL of an aqueous dye solution and then shaken for 24 h in an air bath at 25 °C. The pH was set at 5 and the shaking rate was 200 rpm. Samples were collected at fixed intervals (10, 20, and 30 min and 1, 2, 3, 4, 5, 6, 7, 20, 21, 22 and 24 h), and the concentration of the residual dye in the supernatant was determined. To investigate the effect of initial dye concentration, the same experiment was conducted at other two initial concentrations (viz, 200 mg/L and 500 mg/L). In Fig. 4, the time evolution of the amount of eosin Y adsorbed by EDA-CS from different concentrated dye solutions is displayed. It is clear that an increase in contact time and the initial dye concentration leads to an increase in the adsorption capacity of the dye on EDA-CS. The adsorption amount increases very fast in the first 2 h, equilibrium is approached after 6 h when the adsorption becomes less efficiency with few adsorption sites left. The amount of eosin Y adsorbed at equilibrium increases from 199.8 mg/g to 301.8 mg/g when initial dye concentration increases from 100 mg/L to 500 mg/L. This was expected due to the fact that with higher initial dye concentration, the driving force of the concentration gradient became stronger as well, thus being favorable for dye adsorption (Chiou and Li, 2002).

3.7. Adsorption kinetics

The pseudo-first-order and the pseudo-second order adsorption models were used to test the experimental data. The two kinetic models equations are given as follow:

$$\text{pseudo-first-order equation}: \quad \log(q_e - q_t) = \log q_e - \frac{K_1}{2.303} \tag{3}$$

$$\text{pseudo-second-order equation}: \quad \frac{t}{qt} = \frac{1}{K_2 qe^2} + \frac{t}{qe} \tag{4}$$

where q_e and q_t are the amounts of eosin Y adsorbed on adsorbent (mg/g) at equilibrium time and at time t (min), respectively; K_1 is the rate constant of pseudo-first-order adsorption (min^{-1}), K_2 is the rate constant of second-order adsorption (g/(mg min)).

To testify the applicability of these two models, three initial dye concentrations, 100 mg/L, 200 mg/L and 500 mg/L were applied. Other experiment parameters were identical to those of Section 3.6. The results of the kinetic parameters are listed in Table 1. Based on the correlation coefficients R, the adsorption of eosin Y is best described by the pseudo-second-order equation, suggesting that the rate-limiting step may be the adsorption mechanism but not the mass transport (Kamari, Wan Ngah, Chong, & Cheah, 2009).

3.8. Intraparticle diffusion

In a batch system under rapid stirring, there is a possibility that the transport of the adsorbate from the solution into the bulk of the adsorbent is the rate-controlling step. This possibility was explored using the intraparticle diffusion model (Dŏgan, Abak, &

Table 1
Constants of different rate models.

Initial dye concentration (mg/L)	Pseudo-first-order			Pseudo-second-order			Intraparticle diffusion		
	K_1 (min^{-1})	$q_{e,cal}$ (mg/g)	R^2	K_2 (g/(mg min))	$q_{e,cal}$ (mg/g)	R^2	K_i (mg/(g $min^{1/2}$))	C (mg/g)	R^2
100	4.88×10^{-3}	45.38	0.924	1.903×10^{-4}	204.08	0.99945	9.427	44.37	0.974
200	4.44×10^{-3}	159.29	0.942	7.352×10^{-5}	243.9	0.99786	6.253	76.75	0.9908
500	4.21×10^{-3}	223.54	0.82	4.501×10^{-5}	322.58	0.99622	8.159	89.97	0.982

Alkan, 2009). The initial rate of intraparticle diffusion is given by the following equation:

$$q_t = K_t t^{1\backslash 2} + C \quad (5)$$

where q_t is the amount of dye on the surface of the sorbent at time t (mg/g), K_i is the intraparticle diffusion rate constant (mg/g min$^{1/2}$), t is the time (min) and C is the intercept (mg/g). According to Eq. (5), a plot of q_t versus $t^{1/2}$ should be a straight line when adsorption mechanism follows the sole intraparticle diffusion process.

Some authors have reported that it is essential for the plots to cross the origin if the intraparticle diffusion is the sole rate-limiting step (Crini, Gimbert, Robert, Martel, & Adama, 2008; Rosa, Laranjeira, Riela, & Fávere, 2008). In the present study, the plot does not passed through the origin (see Fig. II in Supplementary data), instead, the plot of q_t against $t^{1/2}$ tends to present a multi-linear behavior, which indicates that two or more steps occur in the adsorption processes, involving instantaneous adsorption on the external surface, intraparticle diffusion or gradual adsorption being the rate-controlled stage, and the final equilibrium stage where the intraparticle diffusion slows down due to the extremely low solute concentration in solution. This phenomenon corresponds to the study of Chiou and Chuang (2006). Since the first stage (external surface adsorption) is completed fast and is less apparent, only the second stage (intraparticle diffusion) and the third stage (equilibrium) are demonstrated. On the other hand, the intercept of the plot reflects the boundary layer effect. Larger the intercept, greater is the contribution of the surface sorption in the rate-limiting step. Corresponding model fitting parameters (shown in Table 1) indicates the adsorption mechanism also follows the intraparticle diffusion process.

3.9. Effect of temperature and initial concentration on the adsorption of EDA-CS

This experiment was carried out as following: 10 mg adsorbent and 20 mL aqueous solution of eosin Y (pH 5) with predetermined initial concentration (50–300 mg/L) was taken in 50 mL plastic bottle. The bottles were agitated (200 rpm) at 25 °C for 24 h, which is expected to exceed the time required to reach equilibrium. At the end of incubation, the beads were separated by filtration and the concentration of the dye in the solution was estimated spectrophotometrically. The same series experiments were carried out at other two temperatures (*viz.*, 35 °C and 45 °C) to investigate the effect of temperature on eosin Y removal.

In Fig. 5, the equilibrium uptake of eosin Y by EDA-CS at three temperatures (25 °C, 35 °C and 45 °C) is plotted as a function of equilibrium dye concentration in the solution.

The results show that adsorption of eosin Y depends on the concentration of the dye. The adsorption capacity increased from 99.95 mg/g to 291.27 mg/g with the increase of eosin Y concentration from 50 mg/L to 500 mg/L at 25 °C. The initial gradient of dye provides the necessary driving force to overcome the resistances to the mass transfer of eosin Y between the aqueous and solid phases (Luo et al., 2010). Temperature also plays a key role in dye adsorption process, that is, when the temperature increases, the equilibrium adsorption falls, indicating the exothermic nature of the adsorption process. Moreover, at higher temperature, the physical interaction between eosin Y and EDA-CS became weaker due to weakening of hydrogen bonds and van der Waals interaction (Chatterjee, Chatterjee, Chatterjee, & Guha, 2007).

3.10. Adsorption isotherm

The adsorption equilibrium isotherm is important for describing the distribution of adsorbate molecules between the liquid and the solid phases at equilibrium. Adsorption equilibrium is established

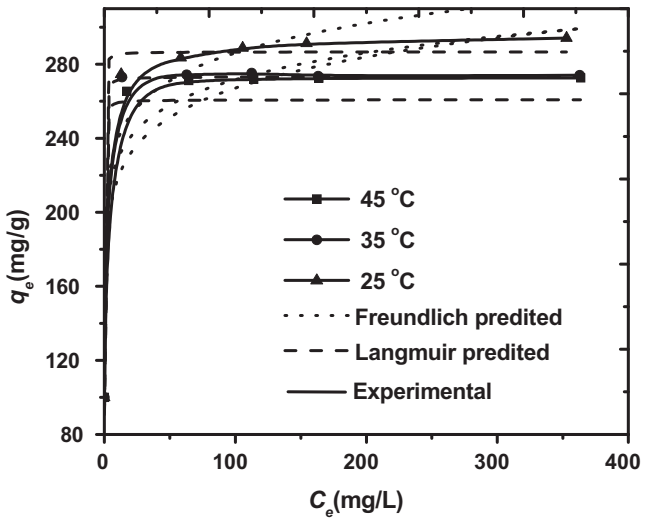

Fig. 5. Variation of equilibrium uptake of eosin Y with temperature at various initial concentrations of eosin Y.

when the amount of dye being adsorbed onto the adsorbent is equal to the amount being desorbed. In the present investigation, the equilibrium data were fitted to the linear form of Freundlich (Eq. (6)) and Langmuir (Eq. (7)) model of adsorption isotherm.

$$\text{Freundlich}: \quad \ln q_e = \ln K_F + \frac{1}{n} \ln C_e \quad (6)$$

$$\text{Langmuir}: \quad \frac{C_e}{q_e} = \frac{1}{K_L q_m} + \frac{C_e}{q_m} \quad (7)$$

where C_e is the remaining dye concentration (mg/L) in solution, q_e the dye concentration (mg/g) in the adsorbent, K_F the Freundlich constant and $1/n$ is the heterogeneity factor. While q_m is the maximum adsorption amount of eosin Y per gram of adsorbent (mg/g) and K_L is the Langmuir adsorption equilibrium constant (L/mg).

Freundlich isotherm supposes that adsorbent surface sites have a spectrum of different binding energies. It describes the adsorption as reversible and not restricted to the monolayer formation. This isotherm does not predict any saturation of the sorbent surface, so dye concentration in the adsorbent will increase with increase of dye concentration in the solution. On the contrary, Langmuir model is valid for monolayer adsorption onto a surface with a finite number of identical sites which are homogeneously distributed over the adsorbent surface. It represents chemisorption on a set of well defined localized sorption sites, supposing that once a particular site of the adsorbent is occupied by an adsorbate molecule, no further adsorption takes place at that site (Kyzas & Lazaridis, 2009). The parameters of Langmuir equation (see Table 1 in Supplementary data) show that the maximum adsorption capacity (q_m) of EDA-CS is 294.12 mg/g at 25 °C, much higher than that of virgin chitosan, which was just about 170.65 mg/g. The correlation coefficients of the isotherms are all higher than 0.99 at the three temperatures, thereby indicating that the Langmuir isotherm fits the equilibrium data very well. On the contrary, the low R^2 values at the test temperatures ($0.74 < R^2 < 0.92$) indicated the poor agreement with Freundlich isotherm.

These results suggest that the surface of EDA modified chitosan is homogeneous and a monolayer of eosin Y covers the surface after adsorption.

The essential characteristics of Langmuir isotherm can be expressed by a dimensionless constant called equilibrium parameter R_L, which is expressed by the following equation:

$$R_L = \frac{1}{1 + K_L C_o} \quad (8)$$

Table 2
Thermodynamic adsorption parameters for the adsorption of eosin Y on EDA-CS.

Temperature (°C)	ΔG° (kJ/mol)	ΔH° (kJ/mol)	ΔS° (J/(mol K))
25	−1.573		
35	−1.321	−5.004	−11.656
45	−1.346		

where K_L is the Langmuir constant as described above and C_o is the initial dye concentration.

The value of R_L indicates the type of the isotherm to be unfavorable ($R_L > 1$), linear ($R_L = 1$), favorable ($0 < R_L < 1$) or irreversible ($R_L = 0$). The degree of favorability is generally related to the irreversibility of the system, giving a qualitative assessment of the interactions between adsorbent and adsorbate. R_L values calculated at different initial dye concentrations (see Table 2 in Supplementary data) are very close to lower acceptable range indicating high degree of irreversibility of the process.

3.11. Thermodynamic of eosin Y adsorption

The thermodynamic parameters including change in free energy (ΔG°), enthalpy (ΔH°) and entropy (ΔS°) were determined using Van't Hoff equation:

$$\ln K_c = \frac{\Delta S^\circ}{R} - \frac{\Delta H^\circ}{RT} \quad (9)$$

$$\Delta G^\circ = -RT \ln K_c \quad (10)$$

$$K_c = \frac{q_e}{C_e} \quad (11)$$

where K_c is the equilibrium constant, q_e is the concentrations of eosin Y adsorbed on solid at equilibrium (mg/g), C_e is the equilibrium concentration of eosin Y in the solution (mg/L), R is the gas constant (8.314 J/(K mol)) and T is the temperature in Kelvin. The values of ΔH and ΔS can be obtained from the slope and intercept of Van't Hoff plot of $\ln K_c$ versus 1/T (see Fig. III in Supplementary data). Plotting of experimental data into linearized form of Van't Hoff can be used to calculate thermodynamic adsorption parameters at solid–solution interface, the results are listed in Table 2.

As can been seen from Table 2, the values of ΔG° are all negative independent of temperature, indicating that the adsorption on EDA-CS is a spontaneous process, which means energy input from outside is not necessary. The decrease in absolute values of ΔG° with increasing temperature suggests that adsorption of eosin Y becomes less favorable at higher temperature.

The negative value of ΔH° (−5.004 kJ/mol) confirms the exothermic nature of adsorption, while the negative value of entropy change (ΔS°) infers a decreased disorder at the solid–solution interface during dyes adsorption. As the temperature goes up, the mobility of dye molecules increases, causing the molecules to escape from the solid phase to the liquid phase, leading to the decreasing adsorption capacity of eosin Y. Similar results were found by Kamari et al. (2009).

4. Conclusions

EDA-CS exhibited interesting sorption properties towards anionic dye eosin Y, due to the high zeta potential contributing to the introduce of great amount of amino groups. The data obtained from adsorption experiments agreed well with Langmuir's isotherm model and the maximum adsorption capacity is 294.12 mg/g at 25 °C, which is much higher than that of chitosan (170.65 mg/g). Kinetics measurements showed that the process was rapid and followed a pseudo-second-order model. This suggests that the rate-limiting step may be the chemisorption not the mass transport. Based on its excellent adsorption performance, it is concluded that EDA-CS could be used as a low-cost and efficient adsorbent for removal of anionic dye (acid dye) from wastewater and has good potential for further application in effluent treatment.

Acknowledgments

The authors thank the financial support provided by the National Science Foundation of China (20874032), by the Key Laboratory of Medicinal Chemical Resources and Molecular Engineering (Ministry of Education) (07109001-17) and by the Project of Curatorial Talents Highland of Guangxi Province (0904).

Appendix A. Supplementary data

Supplementary data associated with this article can be found, in the online version, at doi:10.1016/j.carbpol.2011.01.033.

References

Chatterjee, S., Chatterjee, S., Chatterjee, B. P., & Guha, A. K. (2007). Adsorptive removal of congo red, a carcinogenic textile dye by chitosan hydrobeads: Binding mechanism, equilibrium and Kinetics. *Colloids and Surfaces A: Physicochemical Engineering Aspects*, *299*, 146–152.

Chatterjee, S., Lee, D. S., Lee, M. W., & Woo, S. H. (2009). Congo red adsorption from aqueous solutions by using chitosan hydrogel beads impregnated with nonionic or anionic Surfactant. *Bioresource Technology*, *100*, 3862–3868.

Chiou, M. S., & Chuang, G. S. (2006). Competitive adsorption of dye metanil yellow and RB15 in acid solutions on chemically cross-linked chitosan beads. *Chemosphere*, *62*, 731–740.

Chiou, M. S., & Li, H. Y. (2002). Equilibrium and kinetic modeling of adsorption of reactive dye on cross-linked chitosan beads. *Journal of Hazardous Materials*, *B93*, 233–248.

Chiou, M. S., & Li, H. Y. (2003). Adsorption behavior of reactive dye in aqueous solution on chemical cross-linked chitosan beads. *Chemosphere*, *50*, 1095–1105.

Crini, G. (2006). Non-conventional low-cost adsorbents for dye removal: A review. *Bioresource Technology*, *97*, 1061–1085.

Crini, G., & Badot, P. M. (2008). Application of chitosan, a natural aminopolysaccharide, for dye removal from aqueous solutions by adsorption processes using batch studies: A review of recent literature. *Progress in Polymer Science*, *33*, 399–447.

Crini, G., Gimbert, F., Robert, C., Martel, B., & Adama, O. (2008). The removal of Basic Blue 3 from aqueous solutions by chitosan-based adsorbent: Batch studies. *Journal of Hazardous Materials*, *153*, 96–106.

Dŏgan, M., Abak, H., & Alkan, M. (2009). Adsorption of methylene blue onto hazelnut shell: Kinetics, mechanism and activation parameters. *Journal of Hazardous Materials*, *164*, 172–218.

Du, W. L, Xu, Z. R., Han, X. Y., Xu, Y. L., & Miao, Z. G. (2008). Preparation, characterization and adsorption properties of chitosan nanoparticles for eosin Y as a model anionic dye. *Journal of Hazardous Materials*, *153*, 152–156.

Figueiredoa, S. A., Loureirob, J. M., & Boaventurab, R. A. (2005). Natural waste materials containing chitin as adsorbents for textile dyestuffs: Batch and continuous studies. *Water Research*, *39*, 4142–4152.

Gao, X. Y., Zhou, Y. S., Ma, G. P., Shi, S. Q., Yang, D. Z., Lu, F. M., et al. (2010). A water-soluble photocrosslinkable chitosan derivative prepared by Michael-addition reaction as a precursor for injectable hydrogel. *Carbohydrate Polymers*, *79*, 507–512.

Kamari, A., Wan Ngah, W. S., Chong, M. Y., & Cheah, M. L. (2009). Sorption of acid dyes onto GLA and H_2SO_4 cross-linked chitosan beads. *Desalination*, *249*, 1180–1189.

Kyzas, G. Z., & Lazaridis, N. K. (2009). Reactive and basic dyes removal by sorption onto chitosan derivatives. *Journal of Colloid and Interface Science*, *331*, 32–39.

Luo, P., Zhao, Y. F., Zhang, B., Liu, J. D., Yang, Y., & Liu, J. F. (2010). Study on the adsorption of Neutral Red from aqueous solution onto halloysite nanotubes. *Water Research*, *44*, 1489–1497.

Ngah, W. S. W., Ab Ghani, S., & Kamari, A. (2005). Adsorption behaviour of Fe (II) and Fe (III) ions in queous solution on chitosan and cross-linked chitosan beads. *Bioresource Technology*, *96*, 443–450.

Ong, S. T., Lee, C. K., & Zainal, Z. (2007). Removal of basic and reactive dyes using ethylenediamine modified rice hull. *Bioresource Technology*, *98*, 2792–2799.

Ostrowska-Czubenko, J., & Gierszewska-Drużyńska, M. (2009). Effect of ionic crosslinking on the water state in hydrogel chitosan membranes. *Carbohydrate Polymers*, *77*, 590–598.

Rosa, S., Laranjeira, M. C. M., Riela, H. G., & Fávere, V. T. (2008). Cross-linked quaternary chitosan as an adsorbent for the removal of the reactive dye from aqueous solutions. *Journal of Hazardous Materials*, *155*, 253–260.

Zhang, C., Ping, Q. N., Zhang, H. J., & Shen, J. (2003). Synthesis and characterization of water-soluble O-succinyl-chitosan. *European Polymer Journal*, *39*, 1629–1634.